A THESIS SUBMITTED TO
THE GRADUATE SCHOOL OF NATURAL AND APPLIED SCIENCES
OF ÇANKIRI KARATEKİN UNIVERSITY

SOLUTION OF THE BOHR HAMILTONIAN FOR THE KRATZER POTENTIAL IN THE γ~UNSTABLE REGION

IN PARTIAL FULFILLMENT OF THE REQUIREMENTS
FOR
THE DEGREE OF MASTER OF SCIENCE
IN
PHYSICS

BY

YILMAZ HASSAN MUSTAFA MUSTAFA

ÇANKIRI

2023

SOLUTION OF THE BOHR HAMILTONIAN FOR THE KRATZER POTENTIAL IN THE γ~UNSTABLE REGION

By Yılmaz Hassan Mustafa MUSTAFA

July 2023

We certify that we have read this thesis and that in our opinion it is fully adequate, in scope and in quality, as a thesis for the degree of Master of Science

Advisor **:** Prof. Dr. İlyas İNCİ

Examining Committee Members:

Chairman **:** Prof. Dr. Ali YİĞİT
Physics
Çankırı Karatekin University

Member **:** Prof. Dr. İlyas İNCİ
Physics
Çankırı Karatekin University

Member **:** Asst. Prof. Dr. Harun EROL
Department of Mechatronics
Kayseri University

Approved for the Graduate School of Natural and Applied Sciences

Prof. Dr. Hamit ALYAR
Director of Graduate School

I hereby declare that all information in this document has been obtained and presented in accordance with academic rules and ethical conduct. I also declare that, as required by these rules and conduct, I have fully cited and referenced all material and results that are not original to this work.

Yılmaz Hassan Mustafa MUSTAFA

ABSTRACT

SOLUTION OF THE BOHR HAMILTONIAN FOR THE KRATZER POTENTIAL IN THE γ~UNSTABLE REGION

Yılmaz Hassan Mustafa MUSTAFA

Master of Science in Physics

Advisor: Prof. Dr. İlyas İNCİ

July 2023

Nuclei having structures around the critical point are the main subject of the nuclear structure physicists in recent years. In this thesis, the energy eigenvalue equation of the γ-unstable nuclei is obtained from the solution of the collective Bohr Hamiltonian with the Kratzer potential by using the Nikiforov-Uvarov method. It is known experimentally that nuclei with mass numbers A =100−150 exhibit structures in the γ-unstable region between the U(5) and O(6) limits. For this reason, Pd isotopes with mass numbers ranging from 102 to 116 were selected. Then the resulting equation was tested to find the experimental excitation energy spectra of Pd isotopes. It was found a good agreement between theory and experiment.

2023, 35 pages

Keywords: Kratzer potential, γ-unstable structure, Collective model

ÖZET

γ~ KARARSIZ BÖLGEDE KRATZER POTANSİYELİ İÇİN BOHR HAMİLTONİYENİNİN ÇÖZÜMÜ

Yılmaz Hassan Mustafa MUSTAFA
Fizik, Yüksek Lisans
Tez Danışmanı: Prof. Dr. İlyas İNCİ
Temmuz 2023

Kritik nokta çevresinde yapılara sahip olan çekirdekler, son yıllarda nükleer yapı fizikçilerinin ana konusudur. Bu tezde, γ-kararsız çekirdeklerin enerji özdeğer denklemi, Kratzer potansiyelinin olduğu kollektif Bohr Hamiltoniyeninin Nikiforov-Uvarov yöntemi kullanılarak çözümünden elde edilmiştir. Kütle numaraları A = 100-150 olan çekirdeklerin U(5) ve O(6) sınırları arasındaki γ-kararsız bölgede yapılar sergiledikleri deneysel olarak bilinmektedir. Bu nedenle kütle numaraları 102 ile 116 arasında değişen Pd izotopları seçilmiştir. Daha sonra ortaya çıkan denklem, Pd izotoplarının deneysel uyarılma enerji spektrumlarını bulmak için test edilirdi. Teori ve deney arasında iyi bir uyum bulundu.

2023, 35 sayfa

Anahtar Kelimeler: Kratzer potansiyeli, γ-kararsız yapı, Kollektif model

PREFACE AND ACKNOWLEDGEMENTS

I would like to thank my thesis advisor, Prof. Dr. İlyas İNCİ, for his patience, guidance and understanding.

Yılmaz Hassan Mustafa MUSTAFA

Çankırı-2023

CONTENTS

LIST OF FIGURES

LIST OF TABLES

1. INTRODUCTION

Atomic nuclei are characterized by their shape in equilibrium. While these shapes correspond to stable nuclei in many cases, there are cases where the system experiences a phase transition between two distinct forms and is quite unstable. The problem that arises here is how to define the structure of the nuclei in the phase transition region and especially at the phase transition point. This problem has been investigated within the Interacting Boson Model (IBM) is the basis for the algebraic model (Iachello and Arima 1987, Iachello and Levine 1995). This method relates distinct forms (phases) to some G algebraic structures' dynamic symmetries (Iachello 2001).

One of the most fascinating areas of nuclear physics is the collective motion of the atomic nucleus, which may be studied to better understand the characteristics and behavior of the atomic nucleus and thereby characterize the nuclear structure. Collective motion, a combination of rotational and vibrational motion in the atomic nucleus, is governed by the long-range quadrupole-quadropole interaction that causes deformation and the short-range coupling interaction that favors spherical forms. The harmony of these factors ensures that the atomic nucleus has a certain shape. With the increasing number of nucleons, the deterioration of the balance between these forces causes the atomic nuclei to exhibit shape-phase transition behavior as a function of the number of protons and neutrons that make up it.

Shape phase transitions in atomic nuclei are handled by the Bohr collective model (Bohr 1952), which describes the collective motion of the nucleus, and the IBM, which considers the nucleus as a vibrating bosonic liquid droplet (Iachello and Arima 1987). In both approaches, in the nucleus of the atom; spherical vibrator, axialy symmetric rotor including prolate and oblate deformed structure, and finally non-axially deformed rotor including triaxial (Davydov and Filippov 1958, Davydov and Rostovsky 1959) and γ-unstable (Wilets and Jean 1956) limit structures appear.

A helpful tool for defining the characteristics of many physical systems is dynamic symmetry (nuclei, molecules, atomic structures, etc.). Dynamic symmetry, according to

(Iachello 1979), occurs when the Hamilton operator H can be expressed in terms of the Casimir operators of an algebraic chain $G \supset G' \supset G'' \supset \cdots$. The most noteworthy examples are the vibron model in molecular physics and the dynamical symmetries of the IBM in nuclear physics (Iachello and Arima 1987 ,Iachello and Levine 1995). By examining the algebraic character of the issue, such dynamic symmetries can be quickly identified. All potential dynamical symmetries of algebra G can be discovered by dissecting it into all subalgebraic chains. For instance, in the IBM, three potential dynamic symmetries are denoted by the first subalgebra U(5), SU(3), and SO(6) that emerge in the chain $G \equiv U(6)$. Dynamic symmetries produce all findings for observables in explicit analytical form and are specifically about solvable issues. As a result, it is very helpful in analyzing experimental data and has produced significant breakthroughs (Cizewski *et al.* 1978, Iachello 2000).

The IBM provides an alternative explanation of nuclear collective excitations of an algebraic nature as opposed to geometric models. The many electromagnetic transitions and low-energy collective states of the even-even nuclei might be accurately described by this realistic theoretical model. In the IBM 's first version (IBM-1), nuclei are viewed as systems made up of bosons with angular momentum L=0 (s-bosons) or L=2 (d-bosons) (Iachello and Arima 1987). A Hamiltonian is commonly used to describe the system of bosons up to two-body interactions, where the number of bosons is equal to half the number of valence fermions (N=n/2). The boson number is both rotationally invariant and conserved. The U(6) group structure contains the symmetries of the s and d bosons. Geometrically U(5), SU(3) and O(6) correspond to spherical vibrator, axially symmetric rotor and γ-unstable rotor, respectively (Kotb 2016).

The quantity of protons and neutrons in an atomic nucleus causes phase transitions to occur. These phase changes aren't always of the thermodynamic variety, sometimes they take the form of quantum phase changes at equilibrium between ground-level and low-energy structures. The idea of critical point symmetries, which describes the structure of nuclei in phase transition points, became the focus of a new branch of study as a result (Casten 2006, Iachello 2000, Iachello 2001, Iachello 2003), introduced three new dynamic symmetries that is called E(5), X(5) and Y(5) in his study examining the critical

point behavior of nuclei. E(5), the critical point in the transition from spherical vibrator to γ-unstable (U(5)↔O(6)) shapes, X(5), the critical point between spherical vibrator and axially deformed (U(5)↔SU(3)) shapes point and Y(5) defines the critical point between axially deformed and triaxially deformed shapes. The Z(4) and Z(5) models define the critical point between the axially deformed oblate and the axially deformed prolate ($(SU(3))^{-}$↔SU(3)), and their solutions are obtained by taking γ=(30°) and γ(30°) respectively (Iachello 2001).

The Bohr Hamiltonian has exactly and approximately two types of solutions. The exact Bohr Hamiltonian solution for independent potentials is derived as the model E(5). The potential used in the Bohr differential equation is independent of , and the term depending on the degree of freedom is taken as an infinite square well potential. The model X(5) is obtained as an approximate $\gamma\approx 0^{\circ}$ solution. Another approximate solution is obtained for $\gamma\approx 30^{0}$ called Z(5) (Uçar 2018), five degrees of freedom are taken into account in each of these situations (three Euler angles and three collective variables). The Z(4) model (Bonatsos *et al.* 2005) is an exact solution to the Bohr Hamiltonian and is obtained by considering only four degrees of freedom (β and Euler angles) independent of $\gamma=(30)^{\circ}$.

In order to investigate the structures of nuclei in two different shape-phase transition regions, many studies have been carried out to obtain exact and approximate analytical solutions of the Bohr Hamiltonian by selecting different potentials. For example, Morse (Boztosun *et al.* 2008), Kratzer, Coulomb, Davidson (Fortunato *et al.* 2006, Sobhani and Hassanabadi 2017, Yigitoglu and Bonatsos 2011, Yigitoglu and Gokbulut 2018), Eckart (Naderi and Hassanabadi 2016), Manning-Rosen (Chabab *et al.* 2016), Killingbeck (Sobhani and Hassanabadi 2016) and Sextic (Buganu and Budaca 2015) have been used.

The Kratzer potential was used in the collective Bohr Hamiltonian that describing the even-even nuclei having a γ-unstable structures. The corresponding Schrödinger equation was solved by using a Nikiforov-Uvarov method. The energy eigenvalue equation was obtained in a closed form. To test the resulting formula, *102−116Pd* isotopes have been selected because from the experimental data, these isotopes have γ-unstable structures. By taking into account the experimantal data of these isotopes, first the Kratzer potentail

parameters have been determined. Then for each isotope, excitation energy spectra have obtained and compared with the experimental data. The Nikiforov-Uvarov method is applied for the first time to solve the collective Bohr Hamiltonian with the Kratzer potential in the gamma-unstable region. With this study, one can see that this method gives exactly the same results found by other methods.

2. LITERATURE REVIEW

The atomic nucleus is considered as a quantum system consisting of protons and neutrons in orbits around a common center of mass and interacting with each other primarily by attractive short-range strong interaction (Casten *et al.* 2000, Colò 2020). One of the biggest problems with nuclear structure the goal of physics is to trace the relationship between nuclear structure evolution and nucleon number and to comprehend this phenomenology from both microscopic and macroscopic angles. The emergence of some characteristic excitation spectra in some nuclei has led up to the development of paradigms of the collective model, which deals with the structure of vibrating spherical nuclei, ellipsoidal nuclei that can both vibrate and rotate, and nuclei intermediate between these two nuclear structures. Nuclear structure studies in regions where rapid structural shape phase changes occur, which undergo very sharp changes with the exchange of only two nucleons, are described by quantum phase transitions. The concept of quantum phase transition is concerned with sudden changes in the structure of the equilibrium state or ground state as a function of some variables. Quantum phase transitions in the atomic nucleus reflect rapid structural changes that occur with changes in the number of neutrons or protons (Cejnar 2010).

Typically, it is assumed that the mass in the non-relativistic Schrodinger equation is independent of position. However, certain physical systems should have position-dependent effective masses based on the experimental results. In addition to semiconductor theory, which has utilized effective masses that rely on the spatial coordinates for many years (Morrow 1987, BenDaniel and Duke 1966), this is also true for atomic nuclei, particularly in the collective model proposed by Bohr (Bohr and Mottelson 1953).

The mass does not commute with the momentum if the momentum is position-dependent. It follows that the standard form of kinetic energy can be generalized in several ways, leading to a Hermitian operator. In order to respect hermiticity and have a position-dependent mass, the most generic nonrelativistic Schrodinger equation was proposed in (Von Roos 1983). Another step was taken in (Bagchi *et al.* 2005), who offered a broad

approach by including a parameter, an, in the kinetic energy component. This parameter not only ensures hermiticity but also the precise solvability of the relevant nonrelativistic Schrodinger equation.

Nuclear physicists Jolos and von Brentano used experimental data on spectra and B(E2) transition rates to show that there must be three separate mass coefficients in the low-lying collective bands of well-deformed axially symmetric even-even nuclei (Jolos and Von Brentano 2008). This approach is extended by a mass tensor with deformation-dependent components (Jolos and Von Brentano 2009), and the concept is applicable to nuclei of any shape. Odd nuclei have lately been included in this strategy (Jolos and Von Brentano 2008).

Recent research (Bonatsos *et al.* 2011) has shown that allowing the nuclear mass to depend on the deformation moderates the rate at which the moment of inertia increases with deformation, so resolving a significant problem with the Bohr Hamiltonian (Ring and Schuck 2004). To do this, a Davidson (Davidson 1932) potential has been combined with super symmetric quantum mechanics techniques (Cooper *et al.* 1995) developed in the study of quantum systems with mass depending on the coordinates (Quesne 2007).

It should be noted that the Davidson potential (Davidson 1932), which was first employed to describe molecular spectra, has long been utilized to describe nuclei. It was made clear that it had the group-theoretical structure SU(1,1) SO(5) within the Bohr Hamiltonian, which represents a significant advancement (Rowe and Bahri 1998). As a result of this discovery, the algebraic collective model was created, a method that converges extremely quickly and enables the computation of the transition probabilities and spectra of any kind of nuclear structure (Rowe *et al.* 2009).

Bohr Hamiltonian with a Kratzer potential is a topic of discussion in the current study (Kratzer 1920). Fortunato and Vitturi employed this potential-originally used in molecular physics-to describe nuclei first (Fortunato and Vitturi 2004).

Recently, there has been a lot of interest in the special solving of the Bohr Hamiltonian (Kumar 1972), which represent collective nuclear properties in meaning of the collective variables. This is due to the fact that the critical point symmetries E(5) and X(5), which determine shape phase transitions between rotational nuclei that are vibrational and those that are unstable/prolate deformed, respectively, have just lately been established (Iachello 2001). In good agreement with experiment, such solutions can characterize nuclei spanning the range between different limiting symmetries (Casten and Mc Cutchan 2007). Critical point symmetries, on the other hand, are only applicable to the description of nuclei that are at or near the critical point.

The classical analog of the IBM was the first to identify shape phase transitions in nuclear structure. This model describes collective nuclei in terms of collective bosons of angular momentum zero (s bosons) and two (d bosons) within the framework of a U(6) overall symmetry, possessing U(5) (vibrational), SU(3) (prolate deformed rotational), and O(6) (gamma-unstable) limiting symmetries. It is helpful to position these limiting symmetries at the corners of a symmetry triangle to visualize them as well as the transitions between them. The collective model has been assigned a corresponding triangle. Within the IBM framework, it has been seen that first-order phase transitions can occur between U(5) and SU(3), while second-order phase transitions can occur between U(5) and O(6). The collective model's first and second examples are represented, respectively, by X(5) and E(5).

In this context, the extraordinarily rich data on nuclear excitations, transition rates, and other phenomena have yielded nuclear models based on the concept of symmetry, designed to explain various aspects of the behavior of the atomic nucleus. Mainly divided into two groups, some models describe the collective excitations of the atomic nucleus (rotation and vibration of the deformed ellipsoid) according to the nuclear shape (Bohr and Mottelson 1953), while others consider the nuclear structure focusing on the interaction between nucleons and specific orbits of nucleons. The investigation of the symmetries underlying the behavior of the atomic nucleus is done with algebraic models using conceptually simple group theoretic methods. In general, each of these models is

complementary approaches used to describe different aspects of the behavior of the nucleus.

2.1 Bohr Hamiltonian

Three Euler angles and two collective coordinates are used to form the Bohr Hamiltonian, that present the spectrum and wave function of collective mode is defined as in Equation (2.1) (Bohr 1952).

$$q_1 = \theta_1;\ q_2 = \theta_2;\ q_3 = \theta_3;\ \ q_4 = \beta;\ \ \ q_5 = \gamma \tag{2.1}$$

Kinetic energy in Bohr Hamiltonian is expressed (Bohr 1952) as in Equation (2.2)

$$T = B/2(ds/dt)2 \tag{2.2}$$

The displacement squared is $ds2$ = g$ijdqidqj$. The Hamiltonian is obtained quantum mechanically by the Pauli-Podolsky rule (Podolsky 1928). Equation (2.3) expressed the symmetric matrix.

$$\nabla^2\Phi = \frac{1}{\sqrt{\mathrm{g}}}\partial_i\sqrt{\mathrm{g}}g^{ij}\,\partial_j\Phi \tag{2.3}$$

The symmetric matrix in Equation (2.3) is expressed as in Equation (2.4)

$$g_{ij} = \begin{pmatrix} g_{11} & g_{12} & g_{13} & 0 & 0 \\ g_{21} & g_{22} & 0 & 0 & 0 \\ g_{31} & 0 & g_{33} & 0 & 0 \\ 0 & 0 & 0 & g_{44} & 0 \\ 0 & 0 & 0 & 0 & g_{55} \end{pmatrix} \tag{2.4}$$

As in Equation (2.5), g and gij are the determinant and inverse matrix of g_{ij}, respectively (Sitenko and Tartakovskii 2014).

$$g = \frac{J_1 J_2 J_3}{B^3}\beta^2 \sin^2\theta_2 = 4\beta^8 \sin^2 3\gamma \sin^2\theta_2 \quad (2.5)$$

where J_k's are the moments of inertia given by Equation (2.6)

$$J_k = 4B\beta^2 \sin^2\left(\gamma - k\frac{2\pi}{3}\right) \quad (2.6)$$

Finally, from Equation (2.3), the Bohr Hamiltonian, obtained as functions of the collective variables shows in Equation (2.7)

$$H = -\frac{\hbar^2}{2B_m}\left[\frac{1}{\beta^4}\frac{\partial}{\partial\beta}\beta^4\frac{\partial}{\partial\beta} + \frac{1}{\beta^2 \sin 3\gamma}\frac{\partial}{\partial\gamma}\sin 3\gamma\frac{\partial}{\partial\gamma} - \frac{1}{4\beta^2}\sum_{k=1}^{3}\frac{Q_k^2}{\sin^2\left(\gamma - \frac{2\pi}{3}k\right)}\right] + V(\beta,\gamma) \quad (2.7)$$

where B_m is the mass parameter. The Bohr Hamiltonian is five-dimensional, with the principal deformation coordinates β (deformation coordinate measuring deviation from spherical shape), γ (a measure of deviation from axial symmetry), and $\hat{Q}_k$(k = 1,2,3) components of angular momentum in the real structure as shown in Equations (2.8), (2.9) and (2.10) (Sitenko and Tartakovskii 2014).

$$\hat{Q}_1 = \hat{Q}_x = -i\left(-\frac{\cos\theta_3}{\sin\theta_2}\frac{\partial}{\partial\theta_1} + \sin\theta_3\frac{\partial}{\partial\theta_2} + \cot\theta_2\cos\theta_3\frac{\partial}{\partial\theta_3}\right) \quad (2.8)$$

$$\hat{Q}_2 = \hat{Q}_y = -i\left(-\frac{\sin\theta_3}{\sin\theta_2}\frac{\partial}{\partial\theta_1} + \cos\theta_3\frac{\partial}{\partial\theta_2} - \cot\theta_2\sin\theta_3\frac{\partial}{\partial\theta_3}\right) \quad (2.9)$$

$$\hat{Q}_3 = \hat{Q}_z = -i\frac{\partial}{\partial\theta_3} \quad (2.10)$$

and the collective wave function is defined by Equation (2.11)

$$\Psi(\beta,\gamma,\theta_i) = f(\beta)\Phi^L_{M,K}(\gamma,\theta_i) \quad (2.11)$$

where $\Phi^{L}_{M,K}$ is defined according to Wigner functions $D^{L}_{M,K}(\theta_i)$ as given in Equation (2.12), (Sitenko and Tartakovskii 2014).

$$\Phi^{L}_{M,K}(\gamma,\theta_i) = \sqrt{\frac{2I+1}{16\pi^2(1+\delta_{K,0})}}\, g^{L}_{K}(\gamma)[D^{L}_{M,K}(\theta_i) + (-1)^{L} D^{L}_{M,-K}(\theta_i)] \qquad (2.12)$$

where θ_i (i=1,2,3) Euler angles, $D^{L}_{M,K}(\theta_i)$ Wigner functions of Euler angles, where L is the quantum number representing angular momentum. *M* and *K* are projections of the laboratory constant on the z-axis, the body constant on the z-axis, and the quantum number *L*, respectively (Figure 2.1).

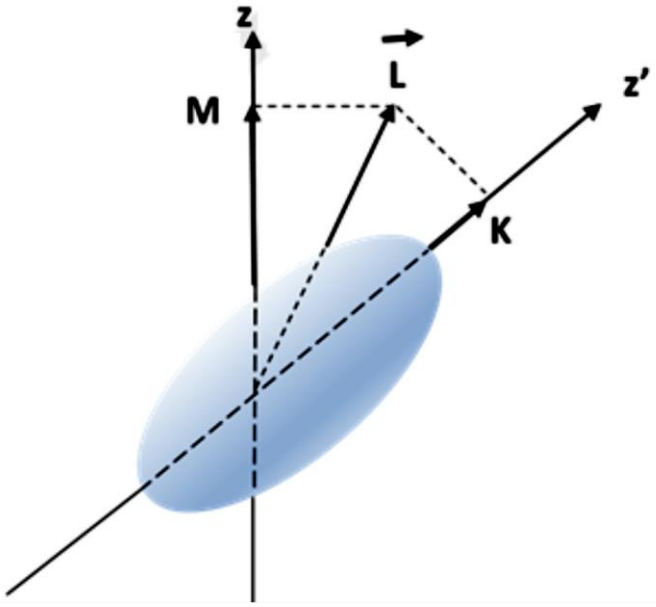

Figure 2.1 Projections of the angular momentum vector

Normalization condition and volume element are given as in Equation (2.13)

$$1 = \int_{\beta=0}^{\infty} \int_{\gamma=0}^{\pi/3} \int_{\theta_1=0}^{2\pi} \int_{\theta_2=0}^{\pi} \int_{\theta_3=0}^{2\pi} \Psi^{*}(\beta,\gamma,\theta_1,\theta_2,\theta_3)\Psi(\beta,\gamma,\theta_1,\theta_2,\theta_3)dv \qquad (2.13)$$
$$dv = \beta^4 d\beta |\sin\ 3\gamma| d\gamma d\theta_1 \sin\ \theta_2 d\theta_2 d\theta_3$$

2.2 Critical Point Symmetries

There are three idealized, known, and commonly used states of the collective even-equivalent nucleus. These cases are the harmonic vibrator, the deformed symmetrical rotor (Bohr and Mottelson 1953) and the γ-unstable (Wilets and Jean 1956). These states of nuclear structure are expressed by the vertices of a symmetry triangle.

These correspond to the terms of the dynamic symmetries U(5), SU(3) and O(6), respectively, in the Interacting boson approximation model (Iachello and Arima 1987). Each of these symmetries has different characteristics. The $R_{4/2}$ energy ratios in spectrum reached by the Bohr Hamiltonian is one of these characteristic features and is a distinctive feature for identifying each nucleus.

The ratio of the energy level with the angular momentum number 4 to the energy level with the angular momentum number 2 gives the energy ratio $R_{4/2}$ as in Equation (2.14)

$$R_{4/2} = \frac{E_4 - E_0}{E_2 - E_0} \tag{2.14}$$

In the framework of the collective model; $R_{4/2}$ = 2.0, 2.5, 3.33. The energy ratios of correspond to the harmonic vibrator, γ-unstable rotor and a deformed axial rotor structures, respectively (Casten 2006). The nuclei surrounding the closed shell have approximately spherical shapes with surface vibrations for $R_{4/2}$ = 2.0. The nucleus shape varies between prolate and oblate when $R_{4/2}$ = 2.5. The potential is independent of since there is no stable shape. The lengths of the three axes vary at every moment. When $R_{4/2}$ = 3.33, closed-shell nuclei with the specified number of distant nucleons have a permanently prolate or oblate distorted shape. They rotate perpendicular to the axis of symmetry in addition to vibrating.

2.3 X(5) Symmetry of the Point Critical

X(5) corresponds to the critical point on the path where the transition from the spherical vibrator to the axial rotor takes place. A first-order phase transition is observed when the potential is minimum (min) ($\gamma = 0°$). First-order phase transition exhibits spherical and deformed phases together, and the ordering parameter is discontinuous. It has two minimum values. The critical point of the phase transition occurs when the potential passes from one minimum to another (Casten 2006).

For a first-order phase transition, coexistence appears as a deformed minimum excited configuration (Coexist curve). If the number of valence nucleons increases, the energy begins to decrease, and a deformed equilibrium state (Def. curve) occurs (Figure 2.2). It shows the critical point (Crit. curve) where the minimums degenerate and is likened to an infinite square well potential. The point of degeneration (Crit. curve) of coexisting shapes is a critical point.

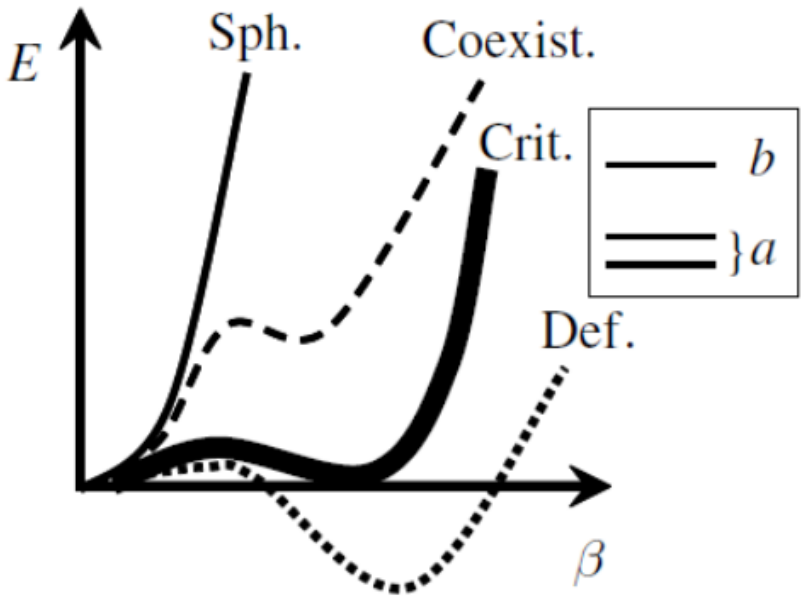

Figure 2.2 The energies at the critical point for the first-order phase transition (Casten and McCutchan 2007)

2.4 E(5) Critical Point Symmetry

The solution between the spherical vibrator and the γ-unstable core structure and corresponding to the critical point is called E(5). A second-order phase transition is observed in this region. Here, the potential is independent of γ (V(γ) = constant), so $V(\beta, \gamma) = U(\beta)$ (Casten 2006). The variable causes the infinite well potential to be the only method for obtaining analytical solutions for the E(5) critical point symmetry β. The energy ratio is $R_{4/2}$ = 2.19. A second-order phase transition occurs when the expected value of β is continuous, the potential does not have two minimum values, and the deformation occurs smoothly, without the coexistence of the two phases. After the phase transition, one has a minimum in the form of a sphere, while the other (the dotted curve) has a minimum in the form of a distorted shape. The crucial point is located in the middle of the curve. There is no relationship between the phases.

2.5 Z(5) Critical Point Symmetry

The path followed to create the Z(5) (Bonatsos *et al.* 2004) critical point symmetry is as follows.

1) Bohr's equation is separated into its variables by taking γ = 30°. Considering the transition from γ = 0° (prolate) to γ = 60° (oblate), it is expected to pass through the triaxial region (0°<γ<60°) and γ = 30° lies in the middle of this transition. There is empirical evidence to support this assumption (Gizon *et al.* 1978).

2) The quantum number K is no longer a good quantum number for γ = 30° (projection of angular momentum to the body-constant $\hat{z}'$ axis). However, the α quantum number and its projection on the body-fixed $\hat{x}'$ axis were found in the triaxial rotor study (Davydov and Filippov 1958, Davydov and Rostovsky 1959).

3) The Z(5) model is created by assuming an infinite well potential in the variable and a harmonic oscillator potential in the variable with γ = 30°.

2.6 Z(4) Critical Point Symmetry

When considering -vibrations, it is believed that the nucleus is a solid structure. The Hamiltonian depends on these four components to work (β, θi) and is expressed as in Equation (2.15)

$$\mathrm{H} = -\frac{\hbar^2}{2\mathrm{B_m}}\left[\frac{1}{\beta^3}\frac{\partial}{\partial\beta}\beta^3\frac{\partial}{\partial\beta} - \frac{1}{4\beta^2}\sum_{\mathrm{k}=1}^{3}\frac{\mathrm{Q_k^2}}{\sin^2\left(\gamma-\frac{2\pi}{3}\mathrm{k}\right)}\right] + \mathrm{U}(\beta) \qquad (2.15)$$

where β and γ are the collective coordinates (Bohr 1952), Qk (k = 1, 2, 3) angular momentum subcomponents and Bm, the mass parameter. This Hamiltonian's exhibits γ a parameter-like behavior rather than a variable-like one. The word "kinetic energy" in Equation (2.15) differs from that in Models E(5) and X(5) because each case has a different number of degrees of freedom.

2.7 Kratzer Potential

The Kratzer potential (Kratzer 1920) has been significant in the development of quantum mechanics. It has been extensively utilized up till now to describe molecular structure and interactions (Leroy and Richard 1970). Kratzer potential is defined as follows by Equation (2.16)

$$V(\beta) = -2D_e\left(\frac{\beta_0}{\beta} - \frac{1}{2}\frac{\beta_0^2}{\beta^2}\right) \qquad (2.16)$$

Here D_e is the dissociation energy and β_0 is the internuclear dissociation equilibrium.

A long-range component of the Kratzer potential is both repellent and alluring. These fragments overlap, resulting in an actual potential gap. For the void form's vibrational and rotational energy eigenvalues to be accurate, this potential is crucial. For the Kratzer potential, when β goes to zero, due to internuclear repulsion, $V(\beta)$ goes to infinity, that

is, the molecule dissociates (Bayrak *et al.* 2007). The Shape of Kratzer potential ($r=\beta$) for different diatomic molecules is shown in Figure 2.3.

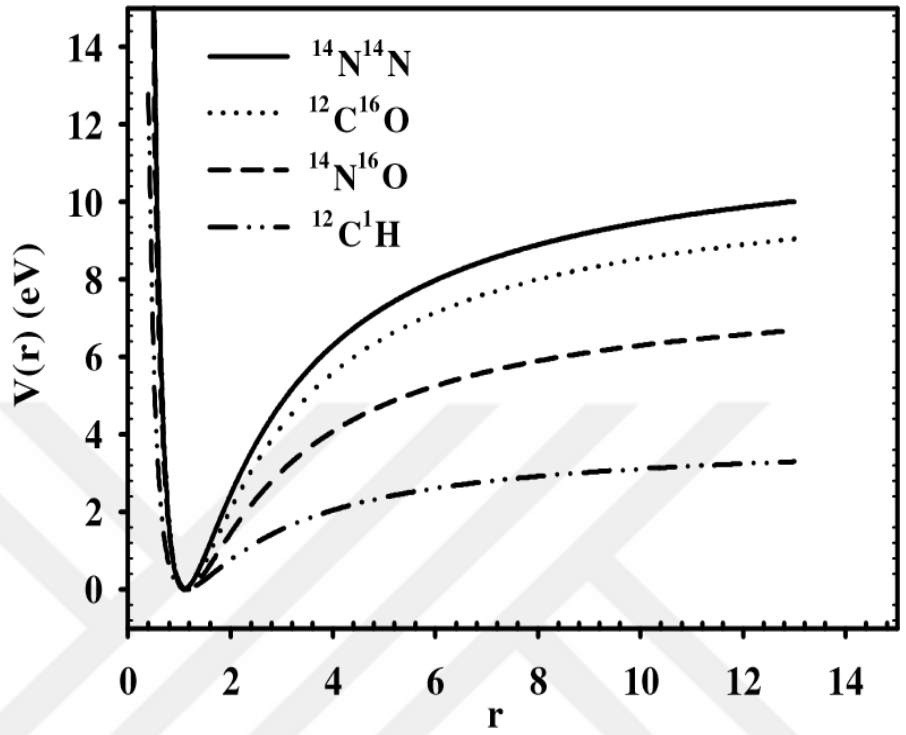

Figure 2.3 Kratzer potential ($r=\beta$) shapes for several diatomic molecules (Berkdemir *et al.* 2006)

3. MATERIALS AND METHODS

In this study, the Bohr and Mottelson collective model, which describes the excitation energy spectrum of even-even nuclei up to 2 MeV, in terms of vibrations and rotations of the nuclear surface will be used. The Bohr Hamiltonian of the system to be studied, is given with.

$$H_B = -\frac{\hbar^2}{2B}\left[\frac{1}{\beta^4}\frac{\partial}{\partial\beta}\beta^4\frac{\partial}{\partial\beta} + \frac{1}{\beta^2\, sin\, 3\gamma}\frac{\partial}{\partial\gamma}sin\, 3\,\gamma\frac{\partial}{\partial\gamma} - \frac{1}{4\beta^2}\sum_{\kappa=1}^{3}\frac{Q_\kappa^2}{sin^2\left(\gamma-\frac{2\pi}{3}\kappa\right)}\right] + V(\beta,\gamma) \quad (3.1)$$

Here, B is the mass parameter, (β,γ) is the collective variables and $V(\beta,\gamma)$ is the potential energy. In the $\gamma\sim$unstable region, the potential energy of the system depends only on the variable β. Different types for this part of the potential potentials can be used. In this study, Kratzer potential defined as below will be used.

$$U_k(\beta) = -2D\left(\frac{\beta_0}{\beta} - \frac{\beta_0^2}{2\beta^2}\right) \quad (3.2)$$

Here $u = \frac{2B}{h^2}$ reduced potential, D indicates the depth at the point where the potential is minimum, and β_0 indicates the location of the point where the potential is minimum.

The Hamiltonian to be obtained using the Kratzer potential will be solved analytically, and the energy eigenvalue equation will be obtained. By using the energy eigenvalue equation, the potential parameters that will theoretically give the most accurate experimental excitation energy spectrum of Pd isotopes will be found.

In the gamma-unstable limit the potential energy *V(β.γ)* depends only on β, *V(β,γ)=U(β).* This means that in this limit, the solution of the gamma-dependent part of the Hamiltonian is constant and the wave function can be written as *Ψ(β,γ,θ)=f(β)ϕ(γ,θ)*

$$\left[\frac{1}{sin3\gamma}\,\frac{\partial}{\partial\gamma}\,sin3\gamma\,\frac{\partial}{\partial\gamma}-\frac{1}{4}\sum_k\frac{Q_k^2}{\sin\left(\gamma-\frac{2\pi}{3}k\right)^2}\right]\phi(\gamma,\theta)=-\hat{\Lambda}^2\,\phi(\gamma,\theta) \tag{3.3}$$

If we substitute Equation (3.3) in (3.1), the hamiltonian (3.4)

$$\left\{\frac{\hbar^2}{2B}\left[\frac{1}{\beta^4}\,\frac{\partial}{\partial\beta}\,\beta^4\,\frac{\partial}{\partial\beta}-\frac{\hat{\Lambda}^2}{\beta^2}\right]+U(\beta)\right\}\,f(\beta)=Ef(\beta) \tag{3.4}$$

Here $\hat{\Lambda}^2$ is given by Casimir operator, $\hat{\Lambda}^2=\tau(\tau+3)$. $\tau=3v_\Delta-\lambda$ and angular momentum (L) takes the following values. $L=\lambda,\lambda+1,\lambda+2,\dots,2\lambda-2,2\lambda$ (It does not take the value of 2λ-1). Now $u(\beta)=\frac{2B}{\hbar^2}\,U(\beta)$ and ε $=\frac{2B}{\hbar^2}\,E$ are the reduced potential and reduced energy, respectively, and the Equation (3.5) becomes:

$$\left\{-\frac{1}{\beta^4}\,\frac{\partial}{\partial\beta}\,\beta^4\,\frac{\partial}{\partial\beta}+\frac{\tau(\tau+3)}{\beta^2}+U(\beta)\right\}f(\beta)=Ef(\beta) \tag{3.5}$$

and by using the Kratzer potential for reduced potential, one gets Equation (3.6), (3.7)

$$u_k=\frac{-2D\beta_0}{\beta}+\frac{2D\beta_0^2}{2\beta^2} \tag{3.6}$$

$$-\frac{1}{\beta^4}\,\frac{\partial}{\partial\beta}\,\beta^4\,\frac{\partial}{\partial\beta}\,f(\beta)+\left(\frac{\tau(\tau+3)}{\beta^2}-\frac{2D\beta_0}{\beta}+\frac{D\beta_0^2}{\beta^2}\right)\,f(\beta)=\varepsilon\,f(\beta) \tag{3.7}$$

Let's arrange the expression $-\frac{1}{\beta^4}\,\frac{\partial}{\partial\beta}\,\beta^4\frac{\partial}{\partial\beta}\,f(\beta)$ in Equation (3.7) as in Equation (3.8)

$$-\frac{1}{\beta^4}\,\frac{\partial}{\partial\beta}\,\beta^4 f\,'(\beta)=-\frac{1}{\beta^4}\left(4\beta^3\,f\,'(\beta)+\beta^4 f\,''(\beta)\right)=-f''(\beta)-\frac{4}{\beta}\,f'(\beta) \tag{3.8}$$

Now let's rewrite Equation (3.7) as in Equation (3.9) and (3.10)

$$-f''(\beta)-\frac{4}{\beta}f'(\beta)+\left(\frac{\tau(\tau+3)+D\beta_0^2}{\beta^2}-\frac{2D\beta_0}{\beta}\right)f(\beta)=\varepsilon f(\beta) \tag{3.9}$$

$$f''(\beta) + \frac{4}{\beta} f'(\beta) + \left(\frac{2D\beta_0 \cdot \beta + \varepsilon\, \beta^2 - \left[\tau(\tau+3) + \boldsymbol{D}\beta_0^2\right]}{\beta^2}\right) f(\beta) \tag{3.10}$$

To simplify the equation, let's say $2D\beta_0$ = A and $\tau(\tau + 3) + D\beta_0^2 = C$, so Equation (3.9) become as in Equation (3.11)

$$f''(\beta) + \frac{4}{\beta} f'(\beta) + \left(\frac{\varepsilon\beta^2 + A\beta - C}{\beta^2}\right) f(\beta) = 0(\tag{3.11}$$

3.1 Nikiforov – Uvarov Method

According to Equation (3.12) that show below

$$\psi''(s) + \frac{\tilde{\tau}(s)}{\sigma(s)} \psi'(s) + \frac{\tilde{\sigma}(s)}{\sigma^2(s)} \psi(s) = 0 \tag{3.12}$$

σ(s) and $\tilde{\sigma}(s)$ can be at most second order, $\tilde{\tau}(s)$ can be at most first order polynomial.

If we compare Equation (3.13) with Equation (3.12) we found that

$$\begin{aligned} &\tilde{\tau}(\beta) = 4 \\ &\sigma(\beta) = \beta \\ &\tilde{\sigma}(\beta) = \varepsilon\beta^2 + A\beta - C \end{aligned} \tag{3.13}$$

According to the N.U method, $\pi(s)$ is defined as in Equation (3.14)

$$\pi(s) = \frac{\sigma'(s) - \tilde{\tau}(s)}{2} \pm \sqrt{\left(\frac{\sigma'(s) - \tilde{\tau}(s)}{2}\right)^2 - \tilde{\sigma}(s) + k\sigma(s)} \tag{3.14}$$

For our solution, this parameter in terms of β variable is illustrated in Equation (3.15)

$$\pi(\beta) = \frac{\sigma'(\beta) - \tilde{\tau}(\beta)}{2} \pm \sqrt{\left(\frac{\sigma'(\beta) - \tilde{\tau}(\beta)}{2}\right)^2 - \tilde{\sigma}(\beta) + k\,\sigma(\beta)} \tag{3.15}$$

and by using the parameters in Equation (3.13), we got Equations (3.16), (3.17), (3.18), (3.19) and (3.20)

$$\sigma(\beta) = \beta,\ \sigma'(\beta) = \frac{d\sigma(\beta)}{d\beta} = 1 \tag{3.16}$$

$$\tilde{\tau}(\beta) = 4 \quad \text{and} \quad \tilde{\sigma}(\beta) = \varepsilon\beta^2 + A\beta + c \tag{3.17}$$

$$\pi(\beta) = \frac{1-4}{2} \pm \sqrt{\left(\frac{1-4}{2}\right)^2 - \varepsilon\beta^2 - A\beta + c + k\beta} \tag{3.18}$$

$$\pi(\beta) = \frac{-3}{2} \pm \sqrt{-\varepsilon\beta^2 + (k-A)\beta + \left(c + \frac{9}{4}\right)} \tag{3.19}$$

$$\pi(\beta) = -\frac{3}{2} \pm \sqrt{-\varepsilon}\sqrt{\beta^2 + \left(\frac{A-k}{\varepsilon}\right)\beta - \left(\frac{c+\frac{9}{4}}{\varepsilon}\right)} \tag{3.20}$$

This expression is also solved so that the discriminant of the equation in the square root is zero, for example, let's say a 2nd order equation $ax^2 + bx + c = 0$. This equation has 2 roots and is found by $x_{1,2} = \frac{-b \pm \sqrt{\Delta}}{2a}$. The discriminant defined by Δ equals $\Delta = b^2 - 4ac$. If $\Delta = 0$ Roots equals $x_{1\prime 2} = -\frac{b}{2a}$ and $ax^2 + bx + c = \left(x + \frac{b}{2a}\right)^2$ is written.

Now in Equation (3.21), the 2nd order polynomial in the square root $\beta^2 + \left(\frac{A-k}{\varepsilon}\right)\beta - \left(\frac{c+9l4}{\varepsilon}\right) = 0$ discriminate Δ of this balancing:

$$\Delta = \left(\frac{A-k}{\varepsilon}\right)^2 - 4\left(\frac{-(c+9/4)}{\varepsilon}\right) = 0 \Rightarrow \left(\frac{A-k}{\varepsilon}\right)^2 = \frac{-4}{\varepsilon}(c+9/4)$$
$$\frac{A-k}{\varepsilon} = \pm\sqrt{-\frac{4}{\varepsilon}(c+9/4)} \Rightarrow A-k = \pm\varepsilon\sqrt{\frac{-4}{\varepsilon}(c+9/4)} \quad (3.21)$$
$$k = A \pm \varepsilon\sqrt{\frac{-4}{\varepsilon}\left(c+\frac{9}{4}\right)}$$
$$k = A \pm \sqrt{-4\varepsilon(c+9/4)}$$

Also, Equation (3.22)

$$k_+ = A + \sqrt{-4\varepsilon(c+9/4)} \text{ and } \quad k_- = A - \sqrt{-4\varepsilon(c+9/4)} \quad (3.22)$$

Here $\varepsilon < 0$ and $-\varepsilon > 0$ (it is bound state). Now let's go back to Equation (3.20)

Since $\Delta = 0$, the expression in the black root as in Equation (3.23):

$$\pi(\beta) = -\frac{3}{2} \pm \sqrt{-\varepsilon}\sqrt{\left(\beta + \frac{(A-k)}{2\varepsilon}\right)^2} \quad (3.23)$$

We now have four values of $\pi(\beta)$ as in Equations (3.24)

$$\left.\begin{aligned}\pi(\beta) &= -\frac{3}{2} + \sqrt{-\varepsilon}\left(\beta + \frac{A-k_+}{2\varepsilon}\right)\\ \pi(\beta) &= -\frac{3}{2} + \sqrt{-\varepsilon}\left(\beta + \frac{A-k_+}{2\varepsilon}\right)\end{aligned}\right\} \quad k = k_+ = A + \sqrt{-4\varepsilon\left(c+\frac{9}{4}\right)}$$
$$\left.\begin{aligned}\pi(\beta) &= -\frac{3}{2} + \sqrt{-\varepsilon}\left(\beta + \frac{A-k_-}{2E}\right)\\ \pi(\beta) &= \frac{-3}{2} - \sqrt{-\varepsilon}\left(\beta + \frac{A-k_-}{2\varepsilon}\right)\end{aligned}\right\} \quad k = k_- = A - \sqrt{-4\varepsilon\left(c+\frac{9}{4}\right)} \quad (3.24)$$

Now the question is, what value of $\pi(\beta)$ in Equation (3.24) will we use? According to the N.U method, it is completed as $\tau(s) = \tilde{\tau}(s) + 2\pi(s)$. In this expression, the derivative of τ(s)' must be $\frac{d\tau(s)}{ds} < 0$. The most appropriate expression to satisfy this condition is the value in Equation (3.24).

$$\pi(\beta) = \frac{-3}{2} - \sqrt{-\varepsilon}\left(\beta + \frac{A-k_-}{2\varepsilon}\right) \tag{3.24}$$

And if $\tilde{\tau}(\beta) = 4$ from Equation (3.13) is used:

$\tau(\beta) = 4 + 2\left(-\frac{3}{2} - \sqrt{-\varepsilon}\left(\beta + \frac{A-k_-}{2\varepsilon}\right)\right)$ and $k_- = A - \sqrt{-4\varepsilon\left(c + \frac{9}{4}\right)}$ if used as in Equation (3.25):

$$\begin{aligned}
&\tau(\beta) = 4 - 3 - 2\sqrt{-\varepsilon})\left(\beta + \frac{A-A+\sqrt{-4\varepsilon(c+9/4)}}{2\varepsilon}\right) \\
&\tau(\beta) = 1 - 2\sqrt{-\varepsilon}\beta - \frac{2\sqrt{-\varepsilon}\sqrt{-4\varepsilon(c+9/4)}}{2\varepsilon} \\
&\tau(\beta) = 1 - 2\sqrt{-\varepsilon}\beta + \frac{2\sqrt{-\varepsilon}\sqrt{-\varepsilon}\sqrt{(4c+9)}}{2(-\varepsilon)} \\
&\tau(\beta) = 1 - 2\sqrt{-\varepsilon}\beta + \sqrt{4c+9}
\end{aligned} \tag{3.25}$$

So according to the N.U method, $k = \lambda - \pi'(s)$ and $\lambda_n = -n\tau'(s) - \frac{n(n-1)}{2}\sigma'(s)$. As seen in Equations (3.26), (3.27), (3.28) and (3.29).

$$k_- = \lambda - \pi'(\beta) \Rightarrow A - \sqrt{-4\varepsilon\left(c + \frac{9}{4}\right)} = \lambda - [-\sqrt{-\varepsilon}] \tag{3.26}$$

$$\lambda = A - \sqrt{-4\varepsilon\left(c + \frac{9}{4}\right)} - 1\sqrt{-\varepsilon} \tag{3.27}$$

$$\lambda_n = -n(-2\sqrt{-\varepsilon}) \tag{3.28}$$

Since $\lambda = \lambda_n$:

$$A - \sqrt{-4\varepsilon(c+\frac{9}{4})} - \sqrt{-\varepsilon} = +n(2\sqrt{-\varepsilon})$$

$-\varepsilon = \epsilon$ if use: $A - \sqrt{4 \in \left(c+\frac{9}{4}\right)} - \sqrt{\epsilon} = 2n\sqrt{\epsilon} \quad (\epsilon > 0)$

$$A - \sqrt{\epsilon}\sqrt{4c+9} - \sqrt{\epsilon} - 2n\sqrt{\epsilon} = 0 \qquad (3.29)$$

$$A = \sqrt{\epsilon}\left(2n+1+\sqrt{4c+9}\right)$$

$$\sqrt{\epsilon} = \frac{A}{2n+1+\sqrt{4c+9}} \qquad \epsilon = \frac{A^2}{(2n+1+\sqrt{4c+9})^2}$$

$$-\varepsilon = \frac{A^2}{(2n+1+\sqrt{4c+5}\,)^2} \qquad \varepsilon = \frac{-A^2}{(2n+1+\sqrt{4c+5}\,)^2}$$

Recall that $A_r = 2D\beta_0$ and $c = \tau(\tau+3) + D\beta_0^2$. Let's substitute it in Equation (3.29) and got Equation (3.30)

$$\varepsilon = \frac{-A^2}{(2n+1+\sqrt{4C+9}))^2} = \frac{-(2D\beta_0)^2}{\left(2n+1+\sqrt{4\tau(\tau+3)+4D\beta_0^2+9}\right)^2}$$

$$\varepsilon = -\frac{(2D\beta_0)^2}{\left(2n+1+2\sqrt{\tau^2+3\tau+\frac{9}{4}+D\beta_0^2}\right)^2} = -\frac{(2D\beta)^2}{\left(2n+1+2\sqrt{((\tau+3/2))^2+D\beta_0^2}\right)^2} \qquad (3.30)$$

$$\varepsilon = -\frac{4(D\beta_0)^2}{4\left(n+\frac{1}{2}+\sqrt{\left(\tau+\frac{3}{2}\right)^2+D\beta_0^2}\right)^2} = -\frac{D^2\beta_0^2}{\left(n+\frac{1}{2}+\sqrt{\left(c+\frac{3}{2}\right)^2+D\beta_0^2}\right)^2}$$

If $A = 2D\beta_0$ and $\frac{A^2}{4} = D^2\beta_0^2$ are substituted for β_0^2, the Equation is (3.30). Equation (3.31) is the desired result.

$$\varepsilon = -\frac{A^2/4}{\left(n+\frac{1}{2}+\sqrt{\left(\tau+\frac{3}{2}\right)^2+D\beta_0^2}\right)^2} \qquad (3.31)$$

This expression has the same results as Equation (3.13) in (Fortunato and Vitturi 2003).

4. RESULTS AND DISCUSSION

Analytical energy eigenvalue corresponding to the gamma-unstable structure having a Kratzer potential was obtained in Equation (3.31) by using the Nikiforov-Uvarov Method. To test the energy eigenvalue equation, we have selected Pd isotopes that experimentaly known as having structures close to gamma-unstable rotor.

As a first step, the experimental data about the excitation energies of these isotopes have been collected form nuclear data sheets. Then these data have written in a Mathematica code which was written to find the best value of the free parameters. After running this program, one gets the Kratzer potential parameters and the quality factor of the fit. In Table 4.1, the best value of the Kratzer potential parameters is shown. From this Table, the quality factor changes from 0.012 to 0.267 which corresponds to ^{108}Pd and ^{112}Pd, respectively.

Table 4.1 Kratzer potential parameters

ISOTOPE	D	β_0	Δ
$^{102}_{46}Pd$	30.1	1.7	0.06501
$^{104}_{46}Pd$	5.1	3.9	0.09149
$^{106}_{46}Pd$	30.5	1.5	0.11258
$^{108}_{46}Pd$	49.9	1.5	0.01157
$^{110}_{46}Pd$	11.5	2.3	0.22606
$^{112}_{46}Pd$	16.5	1.4	0.26662
$^{114}_{46}Pd$	9.1	2.1	0.23990
$^{116}_{46}Pd$	3.0	4.5	0.19962

By using the parameters given in Table 4.1, we have predicted the excitation energy of the Pd isotopes. The energy eigenvalues are the normalized because the theoretical ground state 0^+ energy is not zero. So, it is vital to make good comparison theoretical result with the experimental data. Table 4.2 and Table 4.3 show the Kratzer potential results and the corresponding data.

Table 4.2 Comparison of experimental data with the theoretical results for the $^{102\text{-}108}Pd$.

		$^{102}_{46}Pd$	$^{104}_{46}Pd$	$^{106}_{46}Pd$	$^{108}_{46}Pd$
$E(4_1^+)$	Theo.	2.354	2.339	2.321	2.383
	Exp.	2.293	2.381	2.401	2.415
$E(6_1^+)$	Theo.	3.932	3.878	3.816	4.038
	Exp.	3.794	4.047	4.056	4.081
$E(8_1^+)$	Theo.	5.611	5.491	5.355	5.854
	Exp.	5.414	5.795	5.787	5.871
$E(10_1^+)$	Theo.	7.293	7.082	6.848	7.731
	Exp.	7.175	7.238	6.902	7.720
$E(12_1^+)$	Theo.	8.909	8.588	8.238	9.592
	Exp.	9.084	8.339	7.987	9.586
$E(14_1^+)$	Theo.	10.420	9.975	9.498	11.383
	Exp.	11.031	9.773	9.560	-
$E(16_1^+)$	Theo.	11.080	11.230	10.621	13.067
	Exp.	-	11.439	11.516	-
$E(18_1^+)$	Theo.	13.040	12.340	11.609	14.626
	Exp.	-	13.354	-	-
$E(20_1^+)$	Theo.	14.160	13.330	12.475	16.052
	Exp.	-	-	-	-

Table 4.3 Comparison of experimental data with the theoretical results for the $^{110\text{-}116}Pd$.

		$^{110}_{46}Pd$	$^{112}_{46}Pd$	$^{114}_{46}Pd$	$^{116}_{46}Pd$
$E(4_1^+)$	Theo.	2.302	2.180	2.226	2.302
	Exp.	2.462	2.533	2.560	2.580
$E(6_1^+)$	Theo.	3.751	3.353	3.499	3.750
	Exp.	4.210	4.447	4.506	4.581
$E(8_1^+)$	Theo.	5.217	4.920	4.699	5.215
	Exp.	6.142	4.920	4.896	5.581
$E(10_1^+)$	Theo.	6.612	5.328	5.768	6.610
	Exp.	6.544	5.045	5.958	6.581
$E(12_1^+)$	Theo.	7.890	6.091	6.690	7.886
	Exp.	7.465	5.745	6.202	7.581
$E(14_1^+)$	Theo.	9.031	6.721	7.471	9.026
	Exp.	-	-	-	-
$E(16_1^+)$	Theo.	10.034	7.239	8.128	10.027
	Exp.	-	-	-	-
$E(18_1^+)$	Theo.	10.907	7.665	8.678	10.899
	Exp.	-	-	-	-
$E(20_1^+)$L	Theo.	11.664	8.019	9.139	11.654
	Exp.	-	-	-	-

In these Tables, the energy of states having angular momentum up to 20. Also, one can see that theoretical results are in goodreement with the data up to angular momentum 14.

Furthermore, above this state, the experimental data is not found in the literature. Our study can give idea about the energy of these unknown states.

From Table 4.4 to Table 4.11, we presented the theoretical full excitation spectrum of the Pd isotopes. As known from the E(5) critical point, the all excited states except first 0^+ and 2^+ in each band are degenerate. Then in these tables, only the highest angular momentum (L=2 τ) state corresponding to each τ is given. These energies are also normalized.

Table 4.4 Calculated excitation energy spectrum of $^{102}_{46}Pd$ isotope

PARAMETERS		**ξ = 0**	**ξ = 1**	**ξ = 2**
τ=0	$L=0^+$	0	4.27242	7.51758
τ=1	$L=2^+$	1	5.02475	8.09772
τ=2	$L=4^+$	2.29285	6.05041	8.89311
τ=3	$L=6^+$	3.79408	7.25578	9.83472
τ=4	$L=8^+$	5.41432	8.55144	10.8555
τ=5	$L=10^+$	7.17464	9.86367	11.8988
τ=6	$L=12^+$	9.08363	11.1388	12.9224

Table 4.5 Calculated excitation energy spectrum of $^{104}_{46}Pd$ isotope

PARAMETERS		**ξ = 0**	**ξ = 1**	**ξ = 2**
τ=0	$L=0^+$	0	4.03045	7.05045
τ=1	$L=2^+$	1	4.77204	7.61552
τ=2	$L=4^+$	2.38137	5.77291	8.38312
τ=3	$L=6^+$	4.04725	6.93457	9.28149
τ=4	$L=8^+$	5.79461	8.16618	10.2431
τ=5	$L=10^+$	7.23826	9.3961	11.2134
τ=6	$L=12^+$	8.33918	10.575	12.1533

Table 4.6 Calculated excitation energy spectrum of $^{106}_{46}Pd$ isotope

PARAMETERS		**ξ = 0**	**ξ = 1**	**ξ = 2**
τ=0	$L=0^+$	0	4.8581	8.65272
τ=1	$L=2^+$	1	5.63297	9.26526
τ=2	$L=4^+$	2.4156	6.7097	10.12
τ=3	$L=6^+$	4.0816	8.00589	11.1545

Table 4.6 Calculated excitation energy spectrum of $^{106}_{46}Pd$ isotope (Continued)

PARAMETERS		**ξ = 0**	**ξ = 1**	**ξ = 2**
τ=4	$L=8^+$	5.87181	9.43741	12.3043
τ=5	$L=10^+$	7.72	10.9289	13.5109
τ=6	$L=12^+$	9.56819	12.4198	14.7261

Table 4.7 Calculated excitation energy spectrum of $^{108}_{46}Pd$ isotope

PARAMETERS		**ξ = 0**	**ξ = 1**	**ξ = 2**
τ=0	$L=0^+$	0	4.27242	7.51758
τ=1	$L=2^+$	1	5.02475	8.09772
τ=2	$L=4^+$	2.4156	6.05041	8.89331
τ=3	$L=6^+$	4.0816	7.25578	9.83472
τ=4	$L=8^+$	5.87181	8.55144	10.8555
τ=5	$L=10^+$	7.720	9.86367	11.8986
τ=6	$L=12^+$	9.58662	11.1388	12.9224

Table 4.8 Calculated excitation energy spectrum of $^{110}_{46}Pd$ isotope

PARAMETERS		**ξ = 0**	**ξ = 1**	**ξ = 2**
τ=0	$L=0^+$	0	4.27242	7.51758
τ=1	$L=2^+$	1	5.02475	8.09772
τ=2	$L=4^+$	2.46288	6.05041	8.89311
τ=3	$L=6^+$	4.21051	7.25578	9.83472
τ=4	$L=8^+$	6.14216	8.55144	10.8555
τ=5	$L=10^+$	6.54488	9.86367	11.8988
τ=6	$L=12^+$	7.46542	11.1388	12.9224

Table 4.9 Calculated excitation energy spectrum of $^{112}_{46}Pd$ isotope

PARAMETERS		**ξ = 0**	**ξ = 1**	**ξ = 2**
τ=0	$L=0^+$	0	4.27242	7.51758
τ=1	$L=2^+$	1	5.02475	8.09772
τ=2	$L=4^+$	2.53319	6.05041	8.89311
τ=3	$L=6^+$	4.44766	7.25578	9.83472
τ=4	$L=8^+$	4.92073	8.55144	10.8555
τ=5	$L=10^+$	5.04516	9.86367	11.8988
τ=6	$L=12^+$	5.74558	11.1388	12.9224

Table 4.10 Calculated excitation energy spectrum of $^{114}_{46}Pd$ isotope

PARAMETERS		**ξ = 0**	**ξ = 1**	**ξ = 2**
τ=0	$L=0^+$	0	4.27242	7.51758
τ=1	$L=2^+$	1	5.02475	8.09772
τ=2	$L=4^+$	2.56023	6.05041	8.89311
τ=3	$L=6^+$	4.50646	7.25578	9.83472
τ=4	$L=8^+$	4.89697	8.55144	10.8555
τ=5	$L=10^+$	5.95885	9.86367	11.8988
τ=6	$L=12^+$	6.20276	11.1388	12.9224

Table 4.11 Calculated excitation energy spectrum of $^{116}_{46}Pd$ isotope

PARAMETERS		**ξ = 0**	**ξ = 1**	**ξ = 2**
τ=0	$L=0^+$	0	3.56388	6.15338
τ=1	$L=2^+$	1	4.28173	6.68598
τ=2	$L=4^+$	2.58074	5.22693	7.39339
τ=3	$L=6^+$	4.58191	6.29165	8.199
τ=4	$L=8^+$	5.58191	7.38473	9.03629
τ=5	$L=10^+$	6.58191	8.44178	9.85652
τ=6	$L=12^+$	7.58191	9.42452	10.629

5. CONCLUSIONS AND RECOMMENDATION

This study has presented an innovative use of the Kratzer potential in the collective Bohr Hamiltonian, enabling the calculation of the excitation energy spectra for even-even nuclei with γ-unstable structures. This is the first instance where the Nikiforov-Uvarov (NU) method has been utilized to achieve this outcome. The analytical energy eigenvalue equation that was derived was then employed to forecast the excitation energy spectra of 102-116Pd isotopes. The theoretical values achieved were then juxtaposed with existing experimental data for the studied isotopes. This comparison provided a validation of the Nikiforov-Uvarov method's reliability when applied to this type of nuclear structure research. Notably, our work also resulted in the generation of theoretical energy values previously unrecorded in literature. Consequently, this study will serve as a valuable resource for subsequent experimental research. Over recent years, nuclei structures around the critical point have become the primary focus of nuclear structure physicists. This study contributes to this body of knowledge, providing an energy eigenvalue equation for γ-unstable nuclei, derived from the resolution of the collective Bohr Hamiltonian with the Kratzer potential using the Nikiforov-Uvarov method. This work a specific focused on nuclei with mass numbers A =100−150, known to exhibit γ-unstable region structures between the U(5) and O(6) limits. This informed the selection of Pd isotopes with mass numbers from 102 to 116 for our study. The energy eigenvalue equation was then applied to calculate the experimental excitation energy spectra of these Pd isotopes. The results showed a strong alignment between our theoretical predictions and the existing experimental data, thereby affirming the validity and utility of our approach.

For future work, there are several potential directions that can build upon the findings of this study. Firstly, an extension of this methodology to other isotopes and elements, particularly those in the A =100−150 mass number range with γ-unstable structures, could help to confirm the universality of the approach. Furthermore, the exploration and adaptation of other potential models could enhance the predictive power of the collective Bohr Hamiltonian for the excitation energy spectra. The integration of the Nikiforov-Uvarov method with more advanced computational and mathematical methods could

streamline calculations and possibly uncover more nuanced nuclear structure phenomena. The theoretical energy values that this study has generated also provide a new direction for experimental work, necessitating the development of experimental procedures for their measurement. It would also be intriguing to investigate the transitions between different nuclear structures, such as from spherical to deformed nuclei, to illuminate the process of structural evolution in nuclei. Lastly, fostering interdisciplinary collaborations between theorists and experimentalists could ensure the reciprocal exchange of insights, benefiting both fields of study.

REFERENCES

Bagchi, B., Banerjee, A., Quesne, C. and Tkachuk, V. M. 2005. Deformed shape invariance and exactly solvable Hamiltonians with position-dependent effective mass. Journal of Physics A: Mathematical and General, 38(13): 2929.

Bayrak, O., Boztosun, I. and Ciftci, H. 2007. Exact analytical solutions to the Kratzer potential by the asymptotic iteration method. International Journal of Quantum Chemistry, 107(3): 540-544.

BenDaniel, D. J. and Duke, C. B. 1966. Space-charge effects on electron tunneling. Physical review, 152(2):683.

Berkdemir, C., Berkdemir, A. and Han, J. 2006. Bound state solutions of the Schrödinger equation for modified Kratzer's molecular potential. Chemical Physics Letters, 417(4-6):326-329

Bohr, A. and Mottelson, B R. 1953. Mat-Fys. Medd. K. Dan. Vidensk. Selsk 27.

Bohr, A. 1952. The coupling of nuclear surface oscillations to the motion of individual nucleons. Munksgaard.

Bonatsos, D., Lenis, D., Petrellis, D., Terziev, P. A. and Yigitoglu, I. 2005. γ-rigid solution of the Bohr Hamiltonian for γ= 30° compared to the E (5) critical point symmetry. Physics Letters B, 621(1-2):102-108.

Bonatsos, D., Georgoudis, P. E., Lenis, D., Minkov, N. and Quesne, C. 2011. Bohr Hamiltonian with a deformation-dependent mass term for the Davidson potential. Physical Review C, 83(4): 44321.

Bonatsos, D., Lenis, D., Petrellis, D. and Terziev, P. A. 2004. Z (5): critical point symmetry for the prolate to oblate nuclear shape phase transition. Physics Letters B, 588(3-4):172-179.

Boztosun, I., Bonatsos, D. and Inci, I. 2008. Analytical solutions of the Bohr Hamiltonian with the Morse potential. Physical Review C, 77(4): 044302.

Buganu, P. and Budaca, R. 2015. Analytical solution for the Davydov-Chaban Hamiltonian with a sextic potential for γ= 30∘. Physical Review C, 91(1):014306.

Casten, R. F. 2006. Shape phase transitions and critical-point phenomena in atomic nuclei. Nature Physics, 2(12):811-820.

Casten, R. F. and McCutchan, E. A. 2007. Quantum phase transitions and structural evolution in nuclei. Journal of Physics G: Nuclear and Particle Physics, 34(7): R285.

Casten, R. and Casten, R. F. 2000. Nuclear structure from a simple perspective (23). Oxford University Press on Demand.

Cejnar, P., Jolie, J. and Casten, R. F. 2010. Quantum phase transitions in the shapes of atomic nuclei. Reviews of Modern Physics, 82(3):2155.

Chabab, M., El Batoul, A., Lahbas, A. and Oulne, M. 2016. Electric quadrupole transitions of the Bohr Hamiltonian with Manning–Rosen potential. Nuclear Physics A, 953: 158-175.

Cizewski, J. A., Casten, R. F., Smith, G. J., Stelts, M. L., Kane, W. R., Börner, H. G. and Davidson, W. F. 1978. Evidence for a New Symmetry in Nuclei: The Structure of Pt 196 and the O (6) Limit. Physical Review Letters, 40(3):167.

Cooper, F., Khare, A. and Sukhatme, U. 1995. Supersymmetry and quantum mechanics. Physics Reports, 251(5-6): 267-385.

Colò, G. 2020. Nuclear density functional theory. Advances in Physics: X, 5(1): 1740061.

Davidson, P. M. 1932. Eigenfunctions for calculating electronic vibrational intensities. Proceedings of the Royal Society of London. Series A, Containing Papers of a Mathematical and Physical Character, 135(827): 459-472.

Davydov, A. S. and Filippov, G. F. 1958. Rotational states in even atomic nuclei. Nuclear Physics, 8: 237-249.

Davydov, A. S. and Rostovsky, V. S. 1959. Relative transition probabilities between rotational levels of non-axial nuclei. Nuclear Physics, 12(1): 58-68.

Ermamatov, M. J. and Fraser, P. R. 2011. Rotational-vibrational excited states of axially symmetric nuclei with different mass parameters. Physical Review C, 84(4): 044321.

Fortunato, L. and Vitturi, A. 2003. Analytically solvable potentials for γ-unstable nuclei. Journal of Physics G: Nuclear and Particle Physics, 29(7):1341.

Fortunato, L., De Baerdemacker, S. and Heyde, K. 2006. Solution of the Bohr Hamiltonian for soft triaxial nuclei. Physical Review C, 74(1):014310.

Fortunato, L. and Vitturi, A. 2004. New analytic solutions of the collective Bohr Hamiltonian for a β-soft, γ-soft axial rotor. Journal of Physics G: Nuclear and Particle Physics, 30(5):627.

Gizon, A., Gizon, J., Diamond, R. M. and Stephens, F. S. 1978. Prolate-oblate transition in Nd isotopes. Journal of Physics G: Nuclear Physics, 4(7):L171.

Iachello, F. 1979. Group theoretical methods in physics. Lecture Notes in Physics, edited by A. Böhm (Lange Springer, Berlin, 1979), 94:420.

Iachello, F. 2000. Dynamic symmetries at the critical point. Physical Review Letters, 85(17):3580.

Iachello, F. 2001. Analytic description of critical point nuclei in a spherical-axially deformed shape phase transition. Physical Review Letters, 87(5):052502.

Iachello, F. 2003. Phase transitions in angle variables. Physical review letters, 91(13):132502.

Iachello, F. and Arima, A. 1987. The Interaction Boson Model, Cambridge Univ. Pres., Cambridge.

Iachello, F. and Levine, R. D. 1995. Algebraic theory of molecules. Oxford University Press.

Jolos, R. V. and Von Brentano, P. 2008. Bohr Hamiltonian, mass coefficients, and the structure of well deformed axially symmetric nuclei. Physical Review C, 78(6): 064309.

Jolos, R. V. and Von Brentano, P. 2009. X (5)* model and the N= 90 nuclei. Physical Review C, 80(3):034308.

Kotb, M. 2016. U (5)-SU (3) nuclear shape transition within the interacting boson model applied to dysprosium isotopes. Physics of Particles and Nuclei Letters, 13:451-459.

Kumar, K. 1972. Intrinsic Quadrupole Moments and Shapes of Nuclear Ground States and Excited States. Physical Review Letters 28(4): 249.

Kratzer, A. 1920. Die ultraroten rotationsspektren der halogenwasserstoffe. Zeitschrift für Physik, 3:289-307.

Leroy, R. J. and Richard, B. B.. 1970. Dissociation Energy and Long-range Potential of Diatomic Molecules from Vibrational Spacings of Higher Levels. The Journal of Chemical Physics 52(8): 3869-79.

Morrow, R. A. 1987. Establishment of an effective-mass Hamiltonian for abrupt heterojunctions. Physical Review B, 35(15): 8074.

Naderi, L. and Hassanabadi, H. 2016. Bohr Hamiltonian and the energy spectra of the triaxial nuclei. The European physical journal plus, 131(1):5.

Podolsky, B. 1928. Quantum-mechanically correct form of Hamiltonian function for conservative systems. Physical Review, 32(5):812.

Quesne, C. 2007. Spectrum generating algebras for position-dependent mass oscillator Schrödinger equations. Journal of Physics A: Mathematical and Theoretical, 40(43):13107.

Ring, P. and Schuck, P. 2004. The nuclear many-body problem. Springer Science & Business Media.

Von Roos, O. 1983. Position-dependent effective masses in semiconductor theory. Physical Review B, 27(12):7547.

Rowe, D. J.,and Bahri, C. 1998. Rotation-vibrational spectra of diatomic molecules and nuclei with Davidson interactions. Journal of Physics A: Mathematical and General, 31(21):4947.

Rowe, D. J.,Welsh, T. A., and Caprio, M. A. 2009. Bohr model as an algebraic collective model. Physical Review C, 79(5):054304.

Sitenko, A. G. and Tartakovskii, V. K. 2014. Lectures on the Theory of the Nucleus. Elsevier.

Sobhani, H. and Hassanabadi, H. 2016. Study of Davydov–Chaban approach considering shifted Killingbeck potential for any l-state. Modern Physics Letters A, 31(27): 1650152.

Sobhani, H. and Hassanabadi, H. 2017. Electric quadrupole transitions for some isotopes of Xenon; considering rigidity for γ= 30∘ collective parameter. Nuclear Physics A, 957:177-183.

Uçar, B. 2018. The solution of bohr hamiltonian for γ = 30° with kratzer potential. MSc. Thesis, Tokat Gaziosmanpaşa university, 57 pages, Tokat.

Wilets, L. and Jean, M. 1956. Surface oscillations in even-even nuclei. Physical Review, 102(3):788.

Yigitoglu, I. and Bonatsos, D. 2011. Bohr Hamiltonian with Davidson potential for triaxial nuclei. Physical Review C, 83(1):014303.

Yigitoglu, I. and Gokbulut, M. 2018. Bohr Hamiltonian for γ= 30∘ with Davidson potential. The European Physical Journal Plus, 133(3):129.